






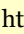
GIS-based landslide susceptibility mapping using hybrid integration approaches of fractal dimension with index of entropy and support vector machine


ZHANG Ting-yu⁴  <https://orcid.org/0000-0001-5589-3318>; e-mail: ztyymy@live.com

HAN Ling^{1*}  <https://orcid.org/0000-0002-9840-4374>;  e-mail: 2016027003@chd.edu.cn

ZHANG Heng¹  <https://orcid.org/0000-0003-0010-5649>; e-mail: xianchdzhang@foxmail.com

ZHAO Yong-hua¹  <https://orcid.org/0000-0001-7437-5911>; e-mail: 252424203@qq.com

LI Xi-an²  <https://orcid.org/0000-0002-0607-9616>; e-mail: 80345022@qq.com

ZHAO Lei³  <https://orcid.org/0000-0003-4190-9635>; e-mail: 75186763@qq.com

* Corresponding author

¹ School of Earth Science and Resources, Chang'an University, Key Laboratory of Degraded and Unutilized Land Remediation Engineering, Ministry of Land and Resources, Shaanxi Provincial Key Laboratory of Land Rehabilitation, Xi'an 710064, China

² School of Geological and Surveying & Mapping Engineering, Chang'an University, Xi'an 710064, China

³ Shaanxi Provincial Land Engineering Construction Group, Xi'an 710075, China

⁴ College of Geology & Environment, Xi'an University of Science and Technology, Xi'an 710054, China

Citation: Zhang TY, Han L, Zhang H, et al. (2019) GIS-based landslide susceptibility mapping using hybrid integration approaches of fractal dimension with index of entropy and support vector machine. *Journal of Mountain Science* 16(6). <https://doi.org/10.1007/s11629-018-5337-z>

© Science Press, Institute of Mountain Hazards and Environment, CAS and Springer-Verlag GmbH Germany, part of Springer Nature 2019

Abstract: The loess area in the northern part of Baoji City, Shaanxi Province, China is a region with frequently landslide occurrences. The main aim of this study is to quantitatively predict the extent of landslides using the index of entropy model (IOE), the support vector machine model (SVM) and two hybrid models namely the F-IOE model and the F-SVM model constructed by fractal dimension. First, a total of 179 landslides were identified and landslide inventory map was produced, with 70% (125) of the landslides which was optimized by 10-fold cross-validation being used for training purpose and the remaining 30% (54) of landslides being used for validation purpose. Subsequently, slope angle, slope aspect, altitude, rainfall, plan curvature, distance to

rivers, land use, distance to roads, distance to faults, normalized difference vegetation index (NDVI), lithology, and profile curvature were considered as landslide conditioning factors and all factor layers were resampled to a uniform resolution. Then the information gain ratio of each conditioning factors was evaluated. Next, the fractal dimension for each conditioning factors was calculated and the training dataset was used to build four landslide susceptibility models. In the end, the receiver operating characteristic (ROC) curves and three statistical indexes involving positive predictive rate (PPR), negative predictive rate (NPR) and accuracy (ACC) were applied to validate and compare the performance of these four models. The results showed that the F-SVM model had the highest PPR, NPR, ACC and AUC values for training and validation datasets, respectively, followed by the F-IOE model.

Received: 24-Dec-2018

1st Revision: 26-Mar-2019

2nd Revision: 07-Apr-2019

Accepted: 05-May-2019

Finally, it is concluded that the F-SVM model performed best in all models, the hybrid model built by fractal dimension has advantages than original model, and can provide reference for local landslide prevention and decision making.

Keywords: GIS; Landslide susceptibility; Hybrid model; Fractal dimension

Introduction

Landslide is a destructive event that often poses a serious threat to human life, property and living environment, and restricts the sustainable development of mankind (Pourghasemi and Rossi 2017). According to statistics, the mortality caused by landslides in developing countries is as high as 95%, and the economic losses caused by landslides account for 1% to 2% of gross national product. As a developing country, mountainous area in China accounts for 70% of total land region. Because of the complex geological and environmental conditions, the strong tectonic activities, and the large-scale engineering construction, the landslides are widely distributed and frequently occurred in China.

Loess is widely distributed in the northwestern of China. Due to the extremely fragile ecology of the Loess Plateau, the loose soil structure, concentrated precipitation and serious soil erosion, the loess area has become the most prone to landslides in China (Chen et al. 2019b). Furthermore, landslides pose a great threat to the development of local social economy and human security. For this reason, landslide prediction is of great significance for landslide control (Guzzetti et al. 1999). However, the traditional field survey is difficult to satisfy the meet of landslide prediction. With the development of geographic information system (GIS) techniques, many statistical approaches were applied for landslide susceptibility mapping, i.e., statistical index (Bui et al. 2011; Aghdam and Pradhan 2016), logistic regression (Aditian et al. 2018; Chen et al. 2019f), certainty factors (Kai et al. 2016; Hong et al. 2017a), analytic hierarchy process (Demir et al. 2013; Abedini and Tulabi 2018), frequency ratio (Vakhshoori and Zare 2016; Sharma and Mahajan 2018), index of entropy (Jaafari et al. 2014; Shirani et al. 2018), and weight of evidence (Ilia and

Tsangaratos 2016; Teerarungsigul et al. 2016). Although statistical approach and GIS techniques can be well combined, and more suitable for large study area, landslide susceptibility mapping is a typical complex and nonlinear problem, therefore the results obtained by statistical approach may not achieve satisfactory accuracy (Bui et al. 2017). Subsequently, many machine learning approaches are introduced, such as artificial neural network (Gorsevski et al. 2016; Saro et al. 2016), kernel logistic regression (Bui et al. 2016; Colkesen et al. 2016; Chen et al. 2018c), random forests (Youssef et al. 2016; Behnia and Blais-Stevens 2018; Ghorbanzadeh et al. 2019), support vector machine (Kavzoglu et al. 2014; Yu and Lu 2018), naive bayes (Pham et al. 2015; Chen et al. 2017b), and decision trees (Chen et al. 2018a,b). The performance of machine learning approach is usually depended on the quality and quantity of training data and is sensitive to parameters in the modeling process (Ghorbanzadeh et al. 2018a). The impact of randomly dividing data, different research scales and different data resolution will affect the training data (Blaschke and Piralilou 2018; Kalantar et al. 2018). Moreover, there is no definitive conclusion about which method is most suitable for studying landslide susceptibility.

In recent years, some hybrid algorithms have made more choices for landslide susceptibility mapping and can also explore more scientific and reasonable results. These new techniques include ANFIS combined with the frequency ratio (Chen et al. 2017a), EBF-fuzzy logic (Bui et al. 2015), fuzzy weight of evidence (Hong et al. 2017b), and set-SVM (Ling et al. 2014). In addition, some scholars use fractal theory to study landslides. The main direction of current research is to use fractal dimension to describe the spatial distribution of landslide (Frattini and Crosta 2013), but almost no research has been done to assess the landslide susceptibility.

Obviously, the assessment methods will have a great impact on the results of landslide susceptibility mapping, and exploring and researching model is considered as an necessary work (Moosavi and Niazi 2016). However, the research on combining fractal dimension with IOE and SVM has not been commonly encountered literatures. Consequently, these two original models (IOE, SVM) and two new hybrid models (F-

IOE, F-SVM) are performed to predict the occurrence of landslide by making landslide susceptibility map at Loess area, Baoji, China.

1 Study Area

The study area is located in the foothill of loess region north part of Baoji city, China, covering an area of approximately 2451 km², and the geographical coordinates are east longitude 107°00'01" - 107°45'08", north latitude 34°29'22" - 34°50'38". It crosses the two major geomorphic units of Loess Platform and the Loess Plateau from the south to the north. The Loess Platform area is 750 – 950 m above sea level, the relative height difference is less than 200 m, while the Loess Plateau region is 900 – 1700 m above sea level, and the relative difference ranges from 100 to 300 m. The rivers in the study area belong to the tributary of the Wei River in the Yellow River basin. The main river is Qian River, the flow of which is northwest to the southeast in study area and finally enters the Wei River, and the total of length of Qian River has reached 28 Km.

The climate of study area is semi-humid climate in the temperate semi-continental monsoon climate, the annual average temperature and the monthly average temperature are 12°C and 25°C, respectively. The average annual precipitation in the study area is 653 mm, and the rainfall period is mainly concentrated from June to September. In the past ten years, the average monthly maximum rainfall was 103 mm, and it

occurred in August. Moreover, the loess is prone to geological disasters because of its collapsibility.

The study area spans three tectonic units from the south to the north across the Loess Plateau, the Ordos Basin and the Qinling Orogenic Belt. There are seven major faults in the study area, of which the F₁-F₅ faults direction is NW-SE, and the F₆-F₇ faults direction is W-E. According to previous records, no destructive earthquakes had occurred in the study area before 2017.

2 Data Used

2.1 Landslide inventory map

Landslide inventory map which includes the information of number, location and size of landslides, is the basis of landslide susceptibility research (Zhang et al. 2018). Based on field survey, previous geological data involving historical landslide data from 1980 to 2017, and aerial remote sensing data, a total of 179 landslides were extracted, including 166 slides, 11 falls and 2 debris flows. All 166 slides belong to shallow landslides, of which 134 slides occurred in soil and 32 slides occur in rock (Hung et al. 2014). The maximum, minimum and average dimension of polygons are 2.2×10⁴ m², 1.1×10³ m², 8.3×10³ m², respectively. Since nearly 90% of the landslides are not more than 10000 m², centroid method (Dai and Lee 2002) was used to transform the polygons to points, and then these points were mapped in the landslide inventory map of study area (Figure 1).

2.2 Preparation of training and validation datasets

In order to build landslide susceptibility model and obtain landslide susceptibility map (LSM), preparation of training and validation datasets is a significant and necessary step (Yalcin et al. 2011). Establishing a landslide susceptibility model must have both positive and negative samples. In this study, all 179 landslide points were used as positive samples. On the other hand, based on analysis of geological data and field observations, the landslides in study area are not likely to occur in areas with slope angles less than 5 degrees, thus these areas were defined as non-landslides areas.

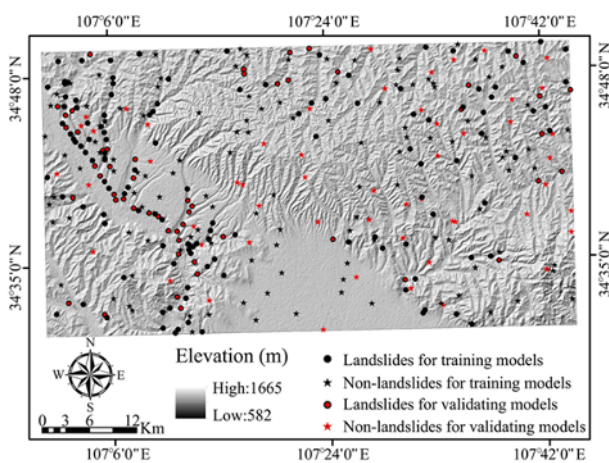


Figure 1 Location of study area and landslide inventory map.

In view of the above facts, the same number of non-landslide points which were used as negative samples were randomly generated in non-landslide area. Then 179 landslide points were randomly divided into two groups at a ratio of 70%/30%, and 179 non-landslide points were split into two groups at the same ratio (Shahabi et al. 2014). Finally, 70% (250) of landslides and non-landslides points were used to train the models, and 30% (108) points were used for validating the models.

There is the fact that one single model can produce high performance just due to randomness (Ghorbanzadeh et al. 2018b). In order to minimize the effects of random selection on the performance of landslide susceptibility model, all landslide points were randomly divided 30 times in a 7/3 ratio, and 10-fold cross-validation was implemented in each group of training datasets. Then the most stable training dataset was retained and applied to detect multicollinearity problem, select conditioning factors and build landslide susceptibility models.

2.3 Analysis of landslide conditioning factors

The occurrence of landslides is affected by a series of conditioning factors such as regional geological environment, hydrology, meteorology and tectonic movement, and the selection and classification of conditioning factors will influence the final accuracy of landslide susceptibility mapping. In present study, a total of 12 internal and external conditioning factors were considered based on field survey and previous studies for landslide susceptibility mapping, which include slope angle, slope aspect, altitude, rainfall, plan curvature, distance to rivers, land use, distance to roads, distance to faults, normalized difference vegetation index (NDVI), lithology, and profile curvature.

The occurrence of landslides is closely to slope angle, and the slope angle directly affects the stress distribution inside the slope and the effective surface (Tehrany et al. 2015). The slope angle information of study area was calculated from DEM data with 30-m resolution and was reclassified into 6 categories with an equal interval of 5° (Appendix 1a). The slope aspect is regarded as another significant factor, which affects the

stability of the slope by affecting the amount of evaporation of the soil, the growth of vegetation, and erosion. The information of slope aspect in study area was also extracted from DEM and was reclassified into 9 groups (Appendix 1b). Similarly, the altitude data extracted from DEM was reclassified into 7 classes with equal interval of 1000 m (Appendix 1c).

Many scholars have found that river erosion plays an important role in landslide occurrence. In present study, distance to rivers was considered as an one of conditioning factors and 5 different buffer zones were generated with equal interval of 100-m (Appendix 1d). The tectonism was also used as an important conditioning factor for landslide susceptibility mapping. The tectonism is not only a necessary condition for a single landslide, but also a direct controlling factor for regional landslides. Therefore, distance to faults was used as a conditioning factor and 5 different buffer zones were generated with equal interval of 1000 m using GIS tools (Appendix 1e). Besides, it was found that road construction required a lot of slope cutting, which is promising to generate potential landslides in the study area. In view of this, distance to roads was considered as another conditioning factor for landslide susceptibility mapping and 4 different buffer zones were generated with equal interval of 100 m (Appendix 1f).

According to the previous literatures, rainfall will greatly influence the stability of landslide. The rainfall data used in this study is the average annual rainfall from 2007 to 2017 provided by the local meteorological observatory. Then rainfall data was divided into 5 classes with equal interval of 150 mm (Appendix 1g). The lithology determines the mechanical strength, weathering resistance, and stress distribution, which in turn influences the stability of the slope and strength of erosion (Chen et al. 2018a). The lithology was reclassified into 6 groups according to the contents shown in Appendix 2 in study area (Appendix 1h). Vegetation also has a significant impact on landslide occurrence. NDVI is always used as a significant indicator to reflect the extent of surface vegetation coverage. In this study, NDVI was calculated from GF-2 multispectral remote sensing images based on ENVI platform and was divided into 5 categories using natural break method (Appendix 1i). In general, land use was often

regarded as one of essential conditioning factors for landslide susceptibility mapping and was divided into 5 groups using GIS tools (Appendix 1j). Plan curvature and profile curvature were calculated by DEM data and were classified into five sections using natural break method (Appendix 1k and 1l), respectively. Finally, based on ArcGIS software, all of these 12 conditioning factors maps were converted into raster images with 30 m spatial resolution.

3 Methodology

In this study, the procedure of landslide susceptibility mapping mainly consists of four parts. The first part was to prepare dataset which included construction of landslide inventory map, analysis of landslide conditioning factors and preparation of training and validation dataset. The second part involved diagnosis of potential multicollinearity problem within landslide conditioning factors, optimization of landslide conditioning factors, and calculation of fractal dimension. The third part was mainly to build four landslide susceptibility models namely the index of entropy model (IOE), index of entropy model based on fractal dimension (F-IOE), support vector machine model (SVM) and the support vector machine model based on fractal dimension (F-SVM). Then the landslide susceptibility maps of study area were derived from aforementioned four models. The fourth part was to evaluate the performance of landslide susceptibility model using statistical indexes, and compare these four models according to the area under receiver operating characteristic curve. The brief presentation of the methods applied in this study is presented in the following paragraphs.

3.1 Multicollinearity diagnosis

Multicollinearity means that the model estimation is distorted or difficult to estimate due to the existence of high correlation between conditioning factors. To detect the existence of multicollinearity, variance inflation factors (VIF) and tolerances were introduced in this study. VIF stands for the ratio of the variance when there is potential multicollinearity problem between the

conditioning factors and the variance when there is no potential multicollinearity problem, and the reciprocal of VIF is the tolerances (Bui et al. 2016; Chen et al. 2019e). In general, the VIF values are proportional to the intensity of the multicollinearity problem between the conditioning factors. When $VIF > 10$ and tolerances < 0.1 , it is considered that a potential multicollinearity problem exists in the dataset (Bai et al. 2010; Chen et al. 2018b).

3.2 Selection of conditioning factors using Information Gain ratio

In landslide susceptibility mapping, not all the conditioning factors have the equal predictive ability in modeling, and it is possible that there may exist noise which will lead to errors in the results. Thus the Information Gain ratio (*IG*) can be calculated to quantitative reflect the contribution of each conditioning factors to landslide susceptibility model, the high *IG* values indicate a higher predictive ability for landslide susceptibility mapping (Ozdemir and Altural 2013). If *IG* values equal to 0, this means the conditioning factor has null predictive ability and should be abandoned (Lombardo et al. 2015). The *IG* values can be calculated as follows:

$$Entropy(D) = - \sum_{k=1}^{|y|} p_k \log_2^{p_k} \quad (1)$$

where *D* is the training dataset, *Entropy* (*D*) denotes the entropy of training dataset, *y* is the number of species in *D*, and *p_k* represents the proportion of category *k* in *D*. Then the training dataset is divided into *D_v* (*v*=1, 2, 3, ... , *m*) using *s* which represents one of the conditioning factors, and calculate the *Gain*(*D*,*s*) by Eq. (2).

$$Gain(D,s) = Entropy(D) - \sum_{v=1}^{|m|} \frac{|D_v|}{D} Entropy(D_v) \quad (2)$$

The *IG* value for conditioning factor *s* is computed as:

$$IG(D,s) = - \frac{Gain(D,s)}{IV(s)} \quad (3)$$

where *IV*(*s*) can be obtained by Eq. (4).

$$IV(s) = - \sum_{v=1}^m \frac{|D_v|}{|D|} \log_2^{\frac{|D_v|}{|D|}} \quad (4)$$

3.3 Fractal dimension

In recent years, many researches showed that the spatial distribution of landslides is not uniform and has 'self-similarity' at different scales, which is consistent with Mandelbrot's fractal theory (Li et al. 2012). Fractal dimension is a parameter used in fractal concept to describe quantitatively fractal characteristics and geometric complexity. In this study, fractal dimension was introduced to represent the degree of clustering of landslides and the complexity of landslide system. There are many methods for measuring the fractal dimension. For small areas, the box-counting techniques are not only simple but also practical. For this reason, subsequent modeling is performed by calculating the fractal dimension using the box-counting techniques.

In current research, the study area was divided into n grids with side length r using ArcGIS software. Then reduce r by a multiple of $1/2$. In this paper, the values of r were 10,000 m, 5000 m, 2500 m, 1250 m, 625 m, and 312.5 m, respectively. Counting the number of grids (N_r) in which the landslide point fall in each grid of different side lengths, and the schematic about the calculation of fractal dimensions was shown in Appendix 3. After that, using a least squares method to fit a straight line as follows:

$$\ln N_r = a + f_j \ln r \quad (5)$$

where a is a parameter, and f_j represents the fractal dimension. Finally, the fractal dimension of each conditioning factors was measured by box-counting techniques which was used as the input data for landslide susceptibility modeling.

3.4 Index of entropy model (IOE) and index of entropy model based on fractal dimension (F-IOE)

As a binary linear statistical analysis model, IOE often appeared in many literatures. The original IOE model calculates the weight of each conditioning factors by counting the frequency ratio of landslides to build landslide susceptibility model. The specific calculation process is as follows:

$$FR_{ij} = \frac{b_{ij}}{a_{ij}} \quad (6)$$

$$P_{ij} = \frac{FR_{ij}}{\sum_{j=1}^{N_j} FR_{ij}} \quad (7)$$

$$H_j = -\sum_{i=1}^{N_j} P_{ij} \log_2 P_{ij}, j = 1, 2, 3, \dots, n \quad (8)$$

$$H_{jmax} = \log_2 N_j \quad N_j \text{ is the number of factors} \quad (9)$$

$$I_j = \frac{H_{jmax} - H_j}{H_{jmax}} \quad (10)$$

$$W_j = I_j \times FR_{ij} \quad (11)$$

where a_{ij} and b_{ij} stand for domain and landslide percentages in the study area, respectively. FR_{ij} is the frequency ratio of landslides, H_j and H_{jmax} is the entropy values, and W_j represents the weight of conditioning factors.

For new hybrid model (F-IOE), the fractal dimension f_j of each factor was used instead of H_j as the modeling data. The final weights of conditioning factors were represented by $F \cdot W_j$.

3.5 Support vector machine model (SVM) and support vector machine model based on fractal dimension (F-SVM)

Support vector machine (SVM) is considered as an efficient supervised learning algorithm for solving binary classification problems. The basic theory of support vector machine model is to find the best separation hyperplane in the feature space, and this hyperplane can maximize the sample interval between landslides and non-landslides data in the training dataset, which can be expressed using mathematical formulas as follows:

$$P = \frac{1}{2} \|w\|^2 \quad (12)$$

Followed by constraints:

$$y_i ((w \times x_i) + b) \geq 1 \quad (13)$$

where b is a constant, and the norm of normal vector on hyperplane is represented by $\|w\|$. The cost function can be defined as Eq.(14) by introducing the Lagrangian multiplier (λ_i).

$$L = \frac{1}{2} \|w\|^2 - \sum_{i=1}^n \lambda_i (y_i ((w \times x_i) + b) - 1) \quad (14)$$

For non-separable case, introducing slack

variables ξ_i (Yilmaz 2010), Eq. (12) and Eq. (13) can be rewritten as follows:

$$y_i((w \times x_i) + b) \geq 1 - \xi_i \quad (15)$$

$$L = \frac{1}{2} \|w\|^2 + C \sum_{i=1}^n \xi_i, \quad (C = -\frac{1}{vn}) \quad (16)$$

where C is penalty coefficient, v represents misclassification and the value of v ranges from 0 to 1. Besides, nonlinear decision boundary can be measured by using a kernel function. In this study, the radial basis function (RBF) was employed for landslide susceptibility modeling and its mathematical formula is as follows:

$$K(x_i, x_j) = \exp(-\delta \|x_i - x_j\|^2), \delta > 0 \quad (17)$$

where δ accounts for the width of the Gaussian kernel function (Pradhan 2013).

Similarly, the fractal dimension f_j was used to replace the original numerical data of each conditioning factor as input data, and then Eq. (12) was applied to classify the input data using hyperplane in high dimensional space. Finally, a new hybrid model (F-SVM) was constructed.

3.6 Statistical validation method

3.6.1 PPR, NPR and ACC

In this study, three kinds of statistical indicators namely positive predictive rate (PPR), negative predictive rate (NPR) and accuracy (ACC) were employed to assess the result of landslide susceptibility mapping. PPR was applied to evaluate the predictive ability of landslide susceptibility models to landslides, and NPR was employed to evaluate the predictive ability of landslide susceptibility models to non-landslides. ACC was employed to measure the accuracy of landslide susceptibility mapping (Sánchez-Reyes et al. 2017). The calculation process of these three statistical indicators is as follows:

$$PPR = \frac{TP}{TP + FP} \quad (18)$$

$$NPR = \frac{TN}{TN + FN} \quad (19)$$

$$ACC = \frac{TP + TN}{TP + TN + FP + FN} \quad (20)$$

Where TP full name is true positive and TN full name is true negative, which represents the number of pixels that are correctly classified. The full name of FP is false positive and the full name of FN is false negative, which represents the number of pixels that are incorrectly classified. In general, if the value of ACC is larger, the accuracy of landslide susceptibility mapping is higher.

3.6.2 The receiver operating characteristic curve (ROC)

The comparative evaluation of the classification results obtained by four models (IOE, F-IOE, SVM, and F-SVM) is a significant part (Pradhan et al. 2014). In this study, the receiver operating characteristic (ROC) curve was introduced to compare these four landslide susceptibility models. The ROC curves reveal the relationship between sensitivity and specificity by using the composition method. It sets several different critical values for continuous variables to calculate a series of sensitivity and specificity values, and then draws the curve with sensitivity as Y-axis and 1-specificity as X-axis (Chen et al. 2019d). The area under the curve abbreviated as AUC was employed to implement the comparison of the performance of each model in the present research. The values of AUC range from 0 to 1 (Chen et al. 2019a,c). If the value of AUC is equal to 1, it indicates that the classification of landslides and non-landslides is completely correct. Conversely, if AUC is equal to 0, the classification is completely wrong. The calculation formula is as follows:

$$\text{Sensitivity} = \text{Y-axis} = \frac{TP}{TP + FN} \quad (21)$$

$$1 - \text{Specificity} = \text{X-axis} = 1 - \frac{TN}{TN + FP} \quad (22)$$

$$AUC = \frac{(\sum TP + \sum TN)}{P + N} \quad (23)$$

where P and N denote the total number of landslides and non-landslides in study area, respectively.

4 Results

4.1 Results of multicollinearity diagnosis

In this study, VIF and TOL were applied to detect the potential multicollinearity problem among conditioning factors. From the calculation results (Table 1), it can be seen that the maximum value of VIF is NDVI (VIF=1.675), and the minimum value of tolerances is land use (tolerances=0.650). VIF and tolerances values for all conditioning factors are not in the range of potential multicollinearity problems (VIF > 10 and tolerances < 0.1), which indicates that there is no multicollinearity problems among these 12 conditioning factors.

Table 1 Variance inflation factors (VIF) and tolerances of each conditioning factor

Conditioning factors	Tolerances	VIF
Slope angle	0.934	1.071
Slope aspect	0.926	1.080
Altitude	0.656	1.525
Distance to rivers	0.908	1.101
Distance to roads	0.877	1.141
Distance to faults	0.916	1.092
NDVI	0.597	1.675
Land use	0.650	1.538
Lithology	0.814	1.228
Rainfall	0.814	1.229
Plan curvature	0.912	1.096
Profile curvature	0.925	1.082

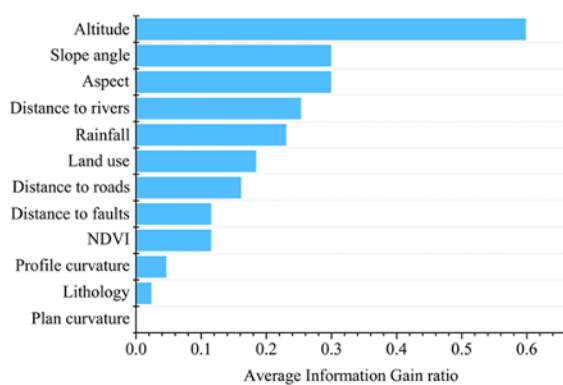


Figure 2 Average Information Gain ratio of each conditioning factor.

4.2 Selection of conditioning factors

In this paper, condition factors are selected by calculating the average merit as the average information gain ratio (AM) using 10-fold cross-validation. From the Figure 2, It can be seen that

altitude has the largest average merit (AM=0.598) in all conditioning factors, followed by slope angle and aspect with the same average merit (AM=0.299), distance to rivers (AM=0.253), rainfall (AM=0.230), land use (AM=0.184), distance to roads (AM=0.184), distance to faults and NDVI (AM=0.115), profile curvature (AM=0.46), and lithology (AM=0.023). However, the average merit of plan curvature is 0, which means plan curvature has null predictive ability for landslide susceptibility modeling and may cause interference. Thus plan curvature is abandoned in subsequent modeling and assessment.

4.3 Calculation of fractal dimension

According to the fractal theory, in order to calculate the fractal dimension of conditioning factors, the spatial distribution of landslides in study area must satisfy the fractal feature (self-similarity). In accordance with the method described above, the spatial fractal dimension of landslide in the study area is obtained using Eq. (5). From the Appendix 4, it can be observed that the spatial fractal dimension of the landslides in the study area is 1.9032 with R^2 of 0.9649, which indicates that the landslides have intense fractal dimension, obvious fractal features, and significant self-similarity. Thus it is meaningful to continue to calculate the spatial fractal dimension of each conditioning factors and the fractal dimension f_j of each factors are presented in Appendix 5.

4.4 Landslide susceptibility mapping based on IOE and F-IOE model

The final calculation data using the IOE and F-IOE models is presented in Appendix 5. As shown in the result, the IOE values and fractal dimension for each conditioning factors have basically the same trend. The maximum W_j (0.3646) belongs to NDVI, followed by land use (0.2462), distance to roads (0.1698), and the minimum W_j (0.0155) belongs to distance to faults. While the maximum $F-W_j$ (0.1388) belongs to profile curvature, followed by NDVI (0.1337), rainfall (0.1319), and the minimum $F-W_j$ (0.0946) belongs to slope aspect. As can be seen from above data, NDVI has a high weight in modeling process of the IOE and F-IOE models. The reason for this phenomenon is

that the serious soil erosion and lack of rain in the study area.

Landslide susceptibility index (LSI) is computed based on the IOE and F-IOE models. The LSI values range from 0 to 1, and the closer to 1 the higher the probability of landslide occurrence vice versa. Finally, the LSI_{IOE} and LSI_{F-IOE} are divided into five intervals to produce landslide susceptibility maps (LSM) which are also divided into five categories by natural break method: very low (0.0940-0.2084) (0.1047-0.1945), low (0.2084-0.2646) (0.1945-0.2783), moderate (0.2646-0.3228) (0.2783-0.3834), high (0.3228-0.3893) (0.3834-0.5022), and very high (0.3893-0.6244) (0.5022-0.7214) (Figures 3(a) and 3(b)).

4.5 Landslide susceptibility mapping based on SVM and F-SVM model

Before building the SVM and F-SVM models based on RBF kernel function, the determination of C and δ is critical for modeling. To acquire

accuracy and stability results, 10-fold cross-validation and a grid-search technique is applied using python software and the final C and δ for SVM and F-SVM are (256, 0.1250) and (512, 0.0165), respectively. Then LSI for the SVM and F-SVM models are computed and the output range from 0 to 1, and the closer to 1 the higher the probability of landslide occurrence, vice versa. Finally, the LSI_{SVM} and LSI_{F-SVM} are divided into five intervals to produce LSM which are also divided into five categories by natural break method: very low (0.0145-0.2459) (0.0740-0.3061), low (0.2459-0.3695) (0.3061-0.3962), moderate (0.3695-0.5161) (0.3962-0.4967), high (0.5161-0.6974) (0.4967-0.6802), and very high (0.6974-0.9983) (0.6802-0.9574) (Figures 3(c) and 3(d)).

4.6 Evaluation and comparison of results

4.6.1 Model performance

The training dataset was applied to assess the

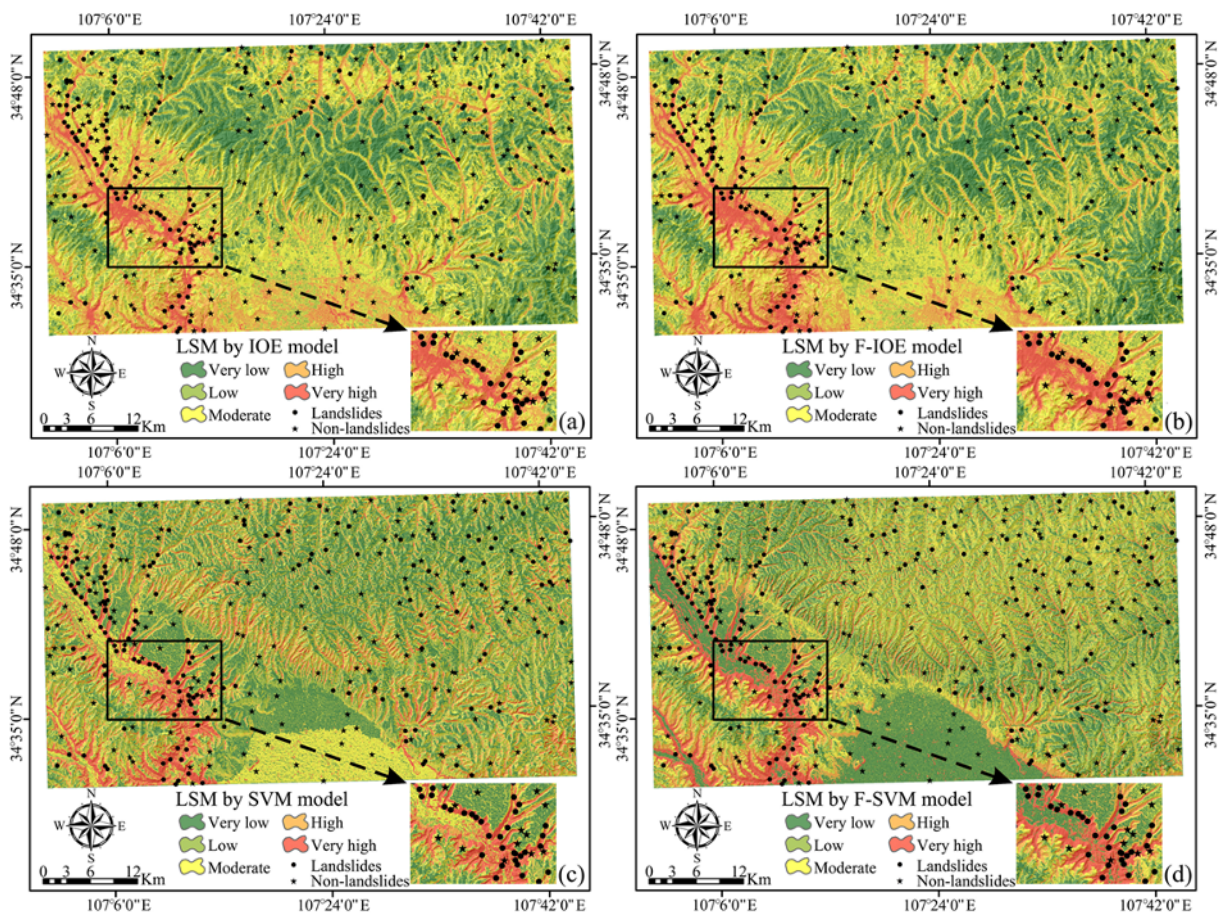


Figure 3 Landslide susceptibility map using a) IOE model; b) F-IOE model; c) SVM model and d) F-SVM model.

performance of landslide susceptibility models based on the three kinds of statistical indicators (*PPR*, *NPR*, and *ACC*), and the results are presented in Table 2. It can be seen from the calculation results of *PPR* and *NPR* that the highest values are the F-SVM model, which are 88.72% and 94.02%, respectively. That is to say, in the current research, the F-SVM model has the highest predictive ability for landslides and non-landslides occurrence among these four models in current research. In terms of *ACC* indicators, the value of the F-SVM model is also the highest (91.20%), followed by the SVM model (89.20%), the F-IOE model (87.60%), and the IOE model (84.80%).

Table 2 Calculation result of statistical indicators for model performance evaluation

Indicators	Models			
	IOE	SVM	F-IOE	F-SVM
True positive	108	113	110	118
True negative	104	110	109	110
False positive	21	15	16	15
False negative	17	12	15	7
<i>PPR</i> (%)	83.72	88.28	87.30	88.72
<i>NPR</i> (%)	85.95	90.16	87.90	94.02
<i>ACC</i> (%)	84.80	89.20	87.60	91.20

Table 3 Calculation result of statistical indicators for model validation evaluation

Indicators	Models			
	IOE	SVM	F-IOE	F-SVM
True positive	48	52	110	118
True negative	47	48	109	110
False positive	7	6	16	15
False negative	6	2	15	7
<i>PPR</i> (%)	87.27	89.66	86.21	92.73
<i>NPR</i> (%)	88.68	96.00	92.00	94.34
<i>ACC</i> (%)	87.96	92.59	88.89	93.52

4.6.2 Model validation

The model validation was completed by using validation dataset and three kinds of statistical indicators, and the calculation results were shown in Table 3. It can be seen from the calculation results of *PPR* and *NPR* that the highest values are the F-SVM model, which are 92.73% and 94.34%, respectively. This indicates that the F-SVM model performs best for the classification of landslides and non-landslides occurrence among these four models in current research. For *ACC* indicators, the value of the F-SVM model is also the highest (93.52%), followed by the SVM model (92.59%), the F-IOE model (88.89%), and the IOE model

(87.96%).

Overall, the performance of these four models is relatively reliable for landslide susceptibility mapping in study area. Furthermore, according to the results of statistical validation method, the F-SVM model got the highest score on all indicators and performs best. Furthermore, both hybrid models have performed better than their original models in the present study.

4.6.3 Model comparison

In this study, the ROC curve was introduced and the *AUC* value was used to compare the landslide susceptibility models. The final results of ROC curves and *AUC* values computed from training and validation datasets for each model were shown in Figures 4(a) and 4(b), respectively. From the ROC curve of training dataset, the F-SVM model shows the highest *AUC* value (0.8527), followed by the SVM model (0.8153), the IOE model (0.8057), and the F-IOE model (0.8054). From the ROC curve of validation dataset, the F-SVM model shows the highest *AUC* value (0.9761) in the same way, followed by the F-IOE model (0.8591), the SVM model (0.7946), and the IOE model (0.7434). As a result, the F-SVM shows the best performance in both training and validation datasets and its *AUC* value from validation dataset is obviously higher than the other models.

5 Discussion

In the current study, based on the landslide inventory map, four landslide susceptibility models namely IOE, F-IOE, SVM, F-SVM models were applied for landslide susceptibility mapping at foothill of loess region north part of Baoji city, China. The overall results confirmed that the two hybrid models presented better classification ability. It is worth noting that although many researchers had use fractal dimension to study landslide in micro and macro (Li et al. 2012; Pourghasemi et al. 2014), there is basically no research on the use of dimension as input data to establish a hybrid model. Since fractal dimension reflects a more realistic spatial distribution of a more realistic landslide, it believes that the reality is chaotic and complex. In addition, the uncertainty represented by fractal dimension is not equal to

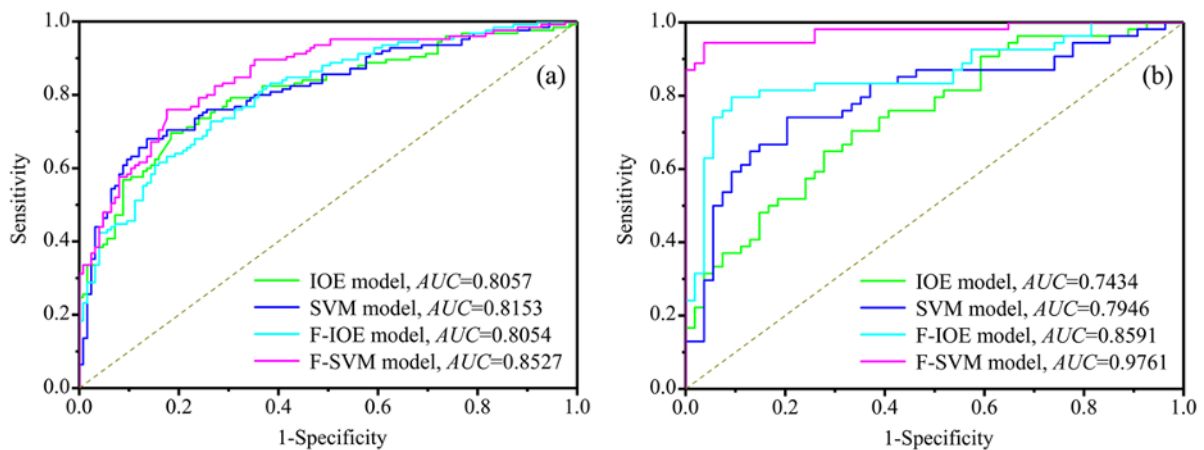


Figure 4 ROC curves for landslide susceptibility models: a) training dataset and b) validation dataset.

randomness, and there is no linear relationship between fractal dimension and conditioning factor. Therefore, it is possible to achieve a better effect than the normal hybrid model by constructing a hybrid model using fractal dimension as input data. On the other hand, the fractal dimension may be used as an index for conditioning factor optimization in the future research.

The difference of scale and data resolution may produce some uncertainty in the process of landslide susceptibility modeling. In the regional landslide susceptibility mapping, it is usually necessary to select a series of conditioning factors with different rates of change on the space-time scale. For example, rainfall and slope angle are the most likely to change, but the lithology is the least likely to change. At large scales, the overall characteristics of conditioning factors in space tend to be more concerned. On the contrary, at small scales, the overall characteristics of conditioning factors in space are often regarded as a constraint, and the information of details is more concerned. As the spatial scale increases, the influence of conditioning factors with high rate of change will decrease or even be erased, while the influence of conditioning factors with slow rate of change will be preserved and even highlighted (Calvello et al. 2013; Lin et al. 2018). All these reasons will lead to uncertainty results of landslide susceptibility mapping. Therefore, we will pay more attention to the influence of scale changes on landslide susceptibility mapping.

From the results of the model performance (section 4.6.1), the *PPR*, *NPR* and *ACC* values of the two hybrid models (F-IOE and F-SVM)

constructed by fractal dimension are higher than their original models (IOE and SVM). Similarly, from the results of the model validation (section 4.6.2), the aforementioned three statistical indexes values of the two hybrid models are also higher than their original models. Furthermore, it can be observed from Figure 4(b) that the *AUC* values of two hybrid models are 0.8591 (F-IOE) and 0.9761 (F-SVM), respectively, which significantly higher than the original models. Therefore, constructing a hybrid model with fractal dimension as input data to research landslide susceptibility in the study area has certain advantages over the original model. However, an insufficient study area is not enough to reflect the universal applicability of the entire method, more case studies need to be constructed.

6 Conclusion

Landslides often threaten the lives of local residents and constrain the development of local economy in the loess area of China. Therefore, quantitative prediction of the area where the landslides occur is necessary, and it has become a hot topic for landslide research. In this study, a total of 179 landslides were identified, 70% landslides were randomly selected for training purpose and the remaining 30% of the landslides were used for validation purpose. Twelve conditioning factors including slope angle, slope aspect, altitude, distance to rivers, distance to roads, distance to faults, NDVI, land use, lithology, rainfall, plan curvature, and profile curvature were selected. The results of multicollinearity diagnosis

indicated that there was no potential multicollinearity problem among conditioning factors. Then the conditioning factors optimization was applied, and plan curvature was abandoned. Two kinds of original classification models namely the IOE and SVM models were constructed. At the same time, the fractal dimension of each conditioning factors was measured and used as the input data to build the two hybrid models namely the F-IOE and F-SVM models. In this study, the final landslide susceptibility map was divided into five classes, such as very low, low, moderate, high and very high using natural break method. In the end, three statistical indexes (*PPR*, *NPR* and *ACC*) were used to evaluate the models performance, and the ROC curve was employed to compare these four models. From the final results, the *ACC* values of these four models were higher than 80% which indicated that the classification results of all models are relatively reliable, and both hybrid models had higher *ACC* values than their original models. In addition, the ROC curves based on

validation dataset showed the similar results, the *AUC* values of F-IOE model and F-SVM model were 0.8591 and 0.9761, respectively, which were higher than the IOE model (0.7434) and SVM model (0.7946). In conclusion, the results in present study prove the hybrid models are feasible for landslide susceptibility mapping in the study area and can provide reference for local landslide prevention and decision making.

Acknowledgements

This research was funded by National Key Research and Development Program of China (Grant No. 2017YFC0504700).

Electronic supplementary material: Supplementary materials (Appendixes 1-5) are available in the online version of this article at <https://doi.org/10.1007/s11629-018-5337-z>.

References

- Abedini M, Tulabi S (2018) Assessing LNRF, FR, and AHP models in landslide susceptibility mapping index: a comparative study of Nojian watershed in Lorestan province, Iran. *Environmental Earth Sciences* 77(11): 405. <https://doi.org/10.1007/s12665-018-7524-1>
- Aditian A, Kubota T, Shinohara Y (2018) Comparison of GIS-based landslide susceptibility models using frequency ratio, logistic regression, and artificial neural network in a tertiary region of Ambon, Indonesia. *Geomorphology* 318: 101-111. <https://doi.org/10.1016/j.geomorph.2018.06.006>
- Aghdam I N, Pradhan B (2016) Landslide susceptibility mapping using an ensemble statistical index (Wi) and adaptive neuro-fuzzy inference system (ANFIS) model at Alborz Mountains (Iran). *Environmental Earth Sciences* 75(7): 1-20. <https://doi.org/10.1007/s12665-015-5233-6>
- Bai S B, Wang J, Lü G N, et al. (2010) GIS-based logistic regression for landslide susceptibility mapping of the Zhongxian segment in the Three Gorges area, China. *Geomorphology* 115(1): 23-31. <https://doi.org/10.1016/j.geomorph.2009.09.025>
- Behnia P, Blais-Stevens A (2018) Landslide susceptibility modelling using the quantitative random forest method along the northern portion of the Yukon Alaska Highway Corridor, Canada. *Natural Hazards* 90(1): 1-20. <https://doi.org/10.1007/s11069-017-3104-z>
- Blaschke T, Pirailiou S T (2018) The Near-Decomposability Paradigm Re-Interpreted for Place-Based GIS. In Proceedings of the 1st Workshop on Platial Analysis (PLATIAL'18), Heidelberg, Germany, 20-21. <https://doi.org/10.5281/zenodo.1472741>
- Bui D T, Bui Q T, Nguyen Q P, et al. (2017) A hybrid artificial intelligence approach using GIS-based neural-fuzzy inference system and particle swarm optimization for forest fire susceptibility modeling at a tropical area. *Agricultural & Forest Meteorology* 233(Complete): 32-44. <https://doi.org/10.1016/j.agrformet.2016.11.002>
- Bui D T, Pradhan B, Revhaug I, et al. (2015) A novel hybrid evidential belief function-based fuzzy logic model in spatial prediction of rainfall-induced shallow landslides in the Lang Son city area (Vietnam). *Geomatics Natural Hazards & Risk* 6(3): 243-271. <https://doi.org/10.1080/19475705.2013.843206>
- Bui D T, Revhaug I, Dick O (2011) Landslide susceptibility analysis in the Hoa Binh province of Vietnam using statistical index and logistic regression. *Natural Hazards* 59(3): 1413-1444. <https://doi.org/10.1007/s11069-011-9844-2>
- Bui D T, Tuan T A, Klempe H, et al. (2016) Spatial prediction models for shallow landslide hazards: a comparative assessment of the efficacy of support vector machines, artificial neural networks, kernel logistic regression, and logistic model tree. *Landslides* 13(2): 361-378. <https://doi.org/10.1007/s10346-015-0557-6>
- Calvello, Michele, Cascini, et al. (2013) Landslide zoning over large areas from a sample inventory by means of scale-dependent terrain units. *Geomorphology* 182(2): 33-48. <https://doi.org/10.1016/j.geomorph.2012.10.026>
- Chen W, Himan S, Zhang S, et al. (2018a) Landslide Susceptibility Modeling Based on GIS and Novel Bagging-Based Kernel Logistic Regression. *Applied Sciences* 8(12): 2540. <https://doi.org/10.3390/app8122540>
- Chen W, Li H, Hou E, et al. (2018b) GIS-based groundwater potential analysis using novel ensemble weights-of-evidence with logistic regression and functional tree models. *Science of the Total Environment* 634: 853. <https://doi.org/10.1016/j.scitotenv.2018.04.055>
- Chen W, Panahi M, Khosravi K, et al. (2019a) Spatial prediction of groundwater potentiality using ANFIS ensembled with Teaching-learning-based and Biogeography-based optimization. *Journal of Hydrology* 572: 435-488. <https://doi.org/10.1016/j.jhydrol.2019.03.013>

- Chen W, Panahi M, Tsangaratos P, et al. (2019b) Applying population-based evolutionary algorithms and a neuro-fuzzy system for modeling landslide susceptibility. *Catena* 172: 212-231. <https://doi.org/10.1016/j.catena.2018.08.025>
- Chen W, Pourghasemi H R, Panahi M, et al. (2017a) Spatial prediction of landslide susceptibility using an adaptive neuro-fuzzy inference system combined with frequency ratio, generalized additive model, and support vector machine techniques. *Geomorphology* 297: 69-85. <https://doi.org/10.1016/j.geomorph.2017.09.007>
- Chen W, Pradhan B, Li S, et al. (2019c) Novel Hybrid Integration Approach of Bagging-Based Fisher's Linear Discriminant Function for Groundwater Potential Analysis. 1-20. <https://doi.org/10.1007/s11053-019-09465-w>
- Chen W, Shahabi H, Shirzadi A, et al. (2018c) Novel hybrid artificial intelligence approach of bivariate statistical-methods-based kernel logistic regression classifier for landslide susceptibility modeling. *Bulletin of Engineering Geology and the Environment*: 1-23. <https://doi.org/10.1007/s10064-018-1401-8>
- Chen W, Shirzadi A, Shahabi H, et al. (2017b) A novel hybrid artificial intelligence approach based on the rotation forest ensemble and naïve Bayes tree classifiers for a landslide susceptibility assessment in Langao County, China. *Geomatics Natural Hazards & Risk*: 1-23. <https://doi.org/10.1080/19475705.2017.1401560>
- Chen W, Sun Z, Han J (2019d) Landslide susceptibility modeling using integrated ensemble weights of evidence with logistic regression and random forest models. *Applied Sciences* 9(1): 171. <https://doi.org/10.3390/app9010171>
- Chen W, Tsangaratos P, Ilia I, et al. (2019e) Groundwater spring potential mapping using population-based evolutionary algorithms and data mining methods. *Science of The Total Environment*: 684. <https://doi.org/10.1016/j.scitotenv.2019.05.312>
- Chen W, Zhao X, Shahabi H, et al. (2019f) Spatial prediction of landslide susceptibility by combining evidential belief function, logistic regression and logistic model tree. *Geocarto International*: 1-25. <https://doi.org/10.1080/10106049.2019.1588393>
- Colkesen I, Sahin E K, Kavzoglu T (2016) Susceptibility mapping of shallow landslides using kernel-based Gaussian process, support vector machines and logistic regression. *Journal of African Earth Sciences* 118(2016): 53-64. <https://doi.org/10.1016/j.jafrearsci.2016.02.019>
- Dai F, Lee C F (2002) Landslides on Natural Terrain: Physical Characteristics and Susceptibility Mapping in Hong Kong. *Mountain Research & Development* 22(1): 40-47. [https://doi.org/10.1659/0276-4741\(2002\)022\[0040:LONT\]2.0.CO;2](https://doi.org/10.1659/0276-4741(2002)022[0040:LONT]2.0.CO;2)
- Demir G, Aytakin M, Akgun A, et al. (2013) A comparison of landslide susceptibility mapping of the eastern part of the North Anatolian Fault Zone (Turkey) by likelihood-frequency ratio; and analytic hierarchy process methods. *Natural Hazards* 65(3): 1481-1506. <https://doi.org/10.1007/s11069-012-0418-8>
- Frattini P, Crosta G B (2013) The role of material properties and landscape morphology on landslide size distributions. *Earth & Planetary Science Letters* 361(1): 310-319. <https://doi.org/10.1016/j.epsl.2012.10.029>
- Ghorbanzadeh O, Blaschke T, Aryal J, et al. (2018a) A new GIS-based technique using an adaptive neuro-fuzzy inference system for land subsidence susceptibility mapping. *Spatial Science*(2): 1-17. <https://doi.org/10.1080/14498596.2018.1505564>
- Ghorbanzadeh O, Blaschke T, Gholamnia K, et al. (2019) Evaluation of Different Machine Learning Methods and Deep-Learning Convolutional Neural Networks for Landslide Detection. *Remote Sensing* 11(2): 196. <https://doi.org/10.3390/rs11020196>
- Ghorbanzadeh O, Rostamzadeh H, Blaschke T, et al. (2018b) A new GIS-based data mining technique using an adaptive neuro-fuzzy inference system (ANFIS) and k-fold cross-validation approach for land subsidence susceptibility mapping. *Natural Hazards* (12). <https://doi.org/10.1007/s11069-018-3449-y>
- Gorsevski P V, Brown M K, Panter K, et al. (2016) Landslide detection and susceptibility mapping using LiDAR and an artificial neural network approach: a case study in the Cuyahoga Valley National Park, Ohio. *Landslides* 13(3): 467-484. <https://doi.org/10.1007/s10346-015-0587-0>
- Guzzetti F, Carrara A, Cardinali M, et al. (1999) Landslide hazard evaluation; a review of current techniques and their application in a multi-scale study, central Italy. *Geomorphology* 31(1-4): 181-216. [https://doi.org/10.1016/S0169-555X\(99\)00078-1](https://doi.org/10.1016/S0169-555X(99)00078-1)
- Hong H, Chen W, Xu C, et al. (2017a) Rainfall-induced landslide susceptibility assessment at the Chongren area (China) using frequency ratio, certainty factor, and index of entropy. *Geocarto International* 32(2): 139-154. <https://doi.org/10.1080/10106049.2015.1130086>
- Hong H, Ilia I, Tsangaratos P, et al. (2017b) A hybrid fuzzy weight of evidence method in landslide susceptibility analysis on the Wuyuan area, China. *Geomorphology* 290: 1-16. <https://doi.org/10.1016/j.geomorph.2017.04.002>
- Hung O, Leroueil S, Picarelli L (2014) The Varnes classification of landslide types, an update. *Landslides* 11(2): 167-194. <https://doi.org/10.1007/s10346-013-0436-y>
- Ilia I, Tsangaratos P (2016) Applying weight of evidence method and sensitivity analysis to produce a landslide susceptibility map. *Landslides* 13(2): 379-397. <https://doi.org/10.1007/s10346-015-0576-3>
- Jaafari A, Najafi A, Pourghasemi H R, et al. (2014) GIS-based frequency ratio and index of entropy models for landslide susceptibility assessment in the Caspian forest, northern Iran. *International Journal of Environmental Science & Technology* 11(4): 909-926. <https://doi.org/10.1007/s12665-016-6162-8>
- Kai C, Dong L, Wei L (2016) Comparison of landslide susceptibility mapping based on statistical index, certainty factors, weights of evidence and evidential belief function models. *Geocarto International*: 1-26. [https://doi.org/10.1016/S0013-7952\(01\)00093-X](https://doi.org/10.1016/S0013-7952(01)00093-X)
- Kalantar B, Pradhan B, Naghibi S A, et al. (2018) Assessment of the effects of training data selection on the landslide susceptibility mapping: a comparison between support vector machine (SVM), logistic regression (LR) and artificial neural networks (ANN). <https://doi.org/10.1080/19475705.2017.1407368>
- Kavzoglu T, Sahin E K, Colkesen I (2014) Landslide susceptibility mapping using GIS-based multi-criteria decision analysis, support vector machines, and logistic regression. *Landslides* 11(3): 425-439. <https://doi.org/10.1007/s10346-013-0391-7>
- Li C, Sun L, Wei L, et al. (2012) Application and verification of a fractal approach to landslide susceptibility mapping. *Natural Hazards* 61(1): 169-185. <https://doi.org/10.1007/s11069-011-9804-x>
- Lin C H, Lin M L, Peng H R, et al. (2018) Framework for susceptibility analysis of layered rock slopes considering the dimensions of the mapping units and geological data resolution at various map scales. *Engineering Geology* 246: 310-325. <https://doi.org/10.1016/j.enggeo.2018.10.004>
- Ling P, Niu R, Bo H, et al. (2014) Landslide susceptibility mapping based on rough set theory and support vector machines: A case of the Three Gorges area, China. *Geomorphology* 204(1): 287-301. <https://doi.org/10.1016/j.geomorph.2013.08.013>
- Lombardo L, Cama M, Conoscenti C, et al. (2015) Binary logistic regression versus stochastic gradient boosted decision trees in assessing landslide susceptibility for multiple-occurring landslide events: application to the 2009 storm event in Messina (Sicily, southern Italy). *Natural Hazards* 79(3): 1621-1648. <https://doi.org/10.1007/s11069-015-1915-3>
- Moosavi V, Niazi Y (2016) Development of hybrid wavelet

- packet-statistical models (WP-SM) for landslide susceptibility mapping. *Landslides* 13(1): 97-114.
<https://doi.org/10.1007/s10346-014-0547-0>
- Ozdemir A, Altural T (2013) A comparative study of frequency ratio, weights of evidence and logistic regression methods for landslide susceptibility mapping: Sultan Mountains, SW Turkey. *Journal of Asian Earth Sciences* 64: 180-197.
<https://doi.org/10.1016/j.jseaes.2012.12.014>
- Pham B T, Bui D T, Pourghasemi H R, et al. (2015) Landslide susceptibility assessment in the Uttarakhand area (India) using GIS: a comparison study of prediction capability of naïve bayes, multilayer perceptron neural networks, and functional trees methods. *Theoretical & Applied Climatology* 122(3): 1-19. <https://doi.org/10.1007/s00704-015-1702-9>
- Pourghasemi H R, Moradi H R, Aghda S M F, et al. (2014) Assessment of fractal dimension and geometrical characteristics of the landslides identified in North of Tehran, Iran. *Environmental Earth Sciences* 71(8): 3617-3626.
<https://doi.org/10.1007/s12665-013-2753-9>
- Pourghasemi H R, Rossi M (2017) Landslide susceptibility modeling in a landslide prone area in Mazandarn Province, north of Iran: a comparison between GLM, GAM, MARS, and M-AHP methods. *Theoretical & Applied Climatology* 130(1-2): 1-25. <https://doi.org/10.1007/s00704-016-1919-2>
- Pradhan B (2013) A comparative study on the predictive ability of the decision tree, support vector machine and neuro-fuzzy models in landslide susceptibility mapping using GIS. *Computers & Geosciences* 51(2): 350-365.
<https://doi.org/10.1016/j.cageo.2012.08.023>
- Pradhan B, Abokharima M H, Jebur M N, et al. (2014) Land subsidence susceptibility mapping at Kinta Valley (Malaysia) using the evidential belief function model in GIS. *Natural Hazards* 73(2): 1019-1042.
<https://doi.org/10.1007/s11069-014-1128-1>
- Sánchez-Reyes U J, Niño-Maldonado S, Barrientos-Lozano L, et al. (2017) Assessment of Land Use-Cover Changes and Successional Stages of Vegetation in the Natural Protected Area Altas Cumbres, Northeastern Mexico, Using Landsat Satellite Imagery. *Remote Sensing* 9(7).
<https://doi.org/10.3390/rs9070712>
- Saro L, Woo J S, Kwan-Young O, et al. (2016) The spatial prediction of landslide susceptibility applying artificial neural network and logistic regression models: A case study of Inje, Korea. *Open Geosciences* 8(1): 117-132.
<https://doi.org/10.1515/geo-2016-0010>
- Shahabi H, Khezri S, Ahmad B B, et al. (2014) Landslide susceptibility mapping at central Zab basin, Iran: A comparison between analytical hierarchy process, frequency ratio and logistic regression models. *Catena* 115(4): 55-70.
<https://doi.org/10.1016/j.catena.2013.11.014>
- Sharma S, Mahajan A K (2018) A comparative assessment of information value, frequency ratio and analytical hierarchy process models for landslide susceptibility mapping of a Himalayan watershed, India. *Bulletin of Engineering Geology & the Environment*(1): 1-18.
<https://doi.org/10.1007/s10064-018-1259-9>
- Shirani K, Pasandi M, Arabameri A (2018) Landslide susceptibility assessment by Dempster-Shafer and Index of Entropy models, Sarkhoun basin, Southwestern Iran. *Natural Hazards*(6): 1-40.
<https://doi.org/10.1007/s11069-018-3356-2>
- Teerarungsikul S, Torizin J, Fuchs M, et al. (2016) An integrative approach for regional landslide susceptibility assessment using weight of evidence method: a case study of Yom River Basin, Phrae Province, Northern Thailand. *Landslides* 13(5): 1151-1165.
<https://doi.org/10.1007/s10346-015-0659-1>
- Tehrany M S, Pradhan B, Jebur M N (2015) Flood susceptibility analysis and its verification using a novel ensemble support vector machine and frequency ratio method. *Stochastic Environmental Research & Risk Assessment* 29(4): 1149-1165.
<https://doi.org/10.1007/s00477-015-1021-9>
- Vakhshoori V, Zare M (2016) Landslide susceptibility mapping by comparing weight of evidence, fuzzy logic, and frequency ratio methods. *Geomatics* 7(5): 1-21.
<https://doi.org/10.1080/19475705.2016.1144655>
- Yalcin A, Reis S, Aydinoglu A C, et al. (2011) A GIS-based comparative study of frequency ratio, analytical hierarchy process, bivariate statistics and logistics regression methods for landslide susceptibility mapping in Trabzon, NE Turkey. *Catena* 85(3): 274-287.
<https://doi.org/10.1016/j.catena.2011.01.014>
- Yilmaz I (2010) Comparison of landslide susceptibility mapping methodologies for Koyulhisar, Turkey: conditional probability, logistic regression, artificial neural networks, and support vector machine. *Environmental Earth Sciences* 61(4): 821-836. <https://doi.org/10.1007/s12665-009-0394-9>
- Youssef A M, Pourghasemi H R, Pourtaghi Z S, et al. (2016) Landslide susceptibility mapping using random forest, boosted regression tree, classification and regression tree, and general linear models and comparison of their performance at Wadi Tayyah Basin, Asir Region, Saudi Arabia. *Landslides* 13(5): 839-856. <https://doi.org/10.1007/s10346-015-0614-1>
- Yu H, Lu Z (2018) Review on landslide susceptibility mapping using support vector machines. *Catena* 165: 520-529.
<https://doi.org/10.1016/j.catena.2018.03.003>
- Zhang T, Han L, Chen W, et al. (2018) Hybrid Integration Approach of Entropy with Logistic Regression and Support Vector Machine for Landslide Susceptibility Modeling. *Entropy* 20(11): 884.
<https://doi.org/10.3390/e20110884>